CHAPTER IV
RESULTS

4.1 Gene expression analysis of CCA fibroblasts

To reduce the genetic background of different patients, the gene expression profile of Cfs was compared to those of two Lfs namely Lf1 and Lf2. Genes with differential expressed levels in Cf compared to Lf1 were 3,560 for 2-fold or more up-regulation and 2,339 for 0.5-fold or less down-regulation (Fig 4-1A and B). The comparison of the Cf to Lf2 were 4,579 and 3,348 for up- and down-regulation, respectively. The common differential genes which are genes altered in their expressions in Cfs when compared to both Lf1 and Lf2 (Cf/Lfs), were 1,466 for up-regulation and 495 for down-regulation.

Arylacetamide deacetylase (*DAC*), procollagen C endopeptidase enhancer 2 (*PCPE2*), serpin peptidase inhibitor transcript variant 2 (*PAI2*) and S100 calcium binding protein A4 (*S100A4*) were predominantly over-expressed at high levels in Cfs (Table 4-1), whereas bone morphogenetic protein 2 (*BMP2*), matrix-remodeling associated 5 (*DKFZp564I1922*), bradykinin receptor B1 (*BRADYB1*), response gene to complement 32 (*RGC32*) and interleukin 24 (*IL-24*) were down-regulated with a high array intensity (Table 4-2).

Using gene ontology to classify biological functions of both common up- and down-regulated genes in Cfs, the result showed that most of common differentially expressed genes in Cfs played roles in controlling cellular metabolism (Table 4-3 and Table 4-4). Additionally, genes encoded for signal transduction molecules were differentially expressed in Cfs and showed 10.9% and 17.8% of total genes for up- and down-regulated genes, respectively. Formyl peptide receptor-like 2 showed the highest up-regulation level among signal transduction related genes whereas *BMP2* was in the first rank of down-regulated gene in this group of biological function. Moreover, genes controlling cell cycle activation including cyclin A1 and cyclin D2 were up-regulated in Cfs, whereas *RGC32* and retinoblastoma 1 showed down-regulation.

For cell proliferation, the result revealed list of up-regulated mitogen-encoded genes including jagged 1 (*JAGL1*), epiregulin (*ER*), and laminin alpha 5 (*LAMA5*) (Table 4-3 and Table 4-4). However, in the down-regulated genes grouping in cell proliferation control, glypican 4 and epidermal growth factor were revealed. Moreover, gene in apoptosis group was taken proportion of gene distribution in up-regulation group (1.6%) much lower than that of down-regulation group (4%).

The raw data of gene expression analysis showing all lists of altered genes can be freely accessed from the Center for Information Biology gene EXpression database (CIBEX) (http://cibex.nig.ac.jp/index.jsp) with experimental accession no. CBX134.

Theoretically, secreted proteins encoding fibroblast-derived genes of which their products can directly expose to cancer cells would have more impact than intracellular protein encoding genes. Hence, the up-regulated genes encoded for secreted proteins mostly classified in groups of extracellular region, proteolysis, and ECM organization/biosynthesis which took up to 11% of total genes were firstly focused (Table 4-3). Among these genes, in addition to the secreted protein encoding genes that act in cell proliferation and motility, 11 genes having several tumorigenic functions were selected for further exploration including a disintegrin and matrix metalloproteinase 12 (*ADAM12*), amphiregulin (*AREG*), angiopoietin 2 (*AGN2*), *ER*, *JAGL1*, *LAMA5*, nephroblastoma over expressed (*NOV*), platelet-derived growth factor-α (*PDGF-A*), periostin (*PN*), reelin (*RL*), and secretogranin 2 (*SCG2*) (Fig 4-1A).

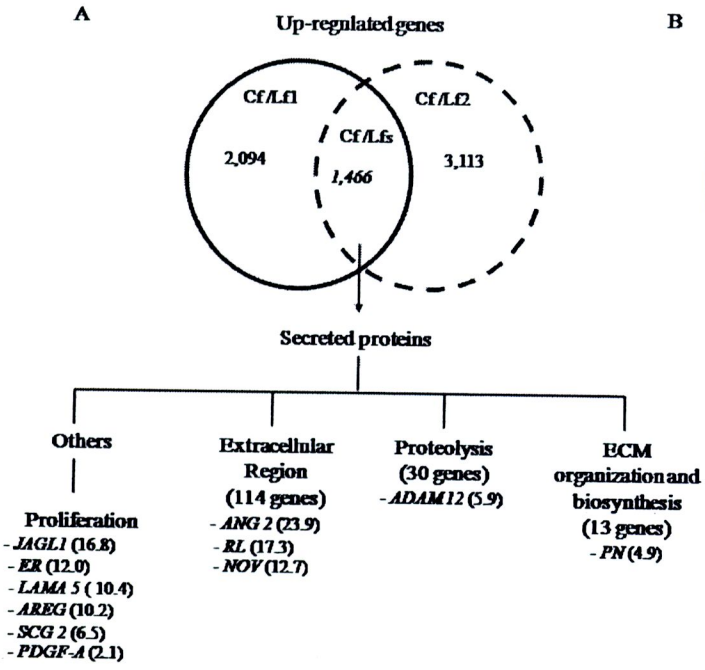

Figure 4-1 Genome wide expression analysis of Cf compared to Lfs. A Vane diagram showed common up-regulated genes (A) and common down-regulated genes (B) in Cf (Cf/Lfs). In this study, eleven genes encoded secreted proteins involved in induction of epithelial cell tumorigenesis including proliferation, invasion, metastasis and angiogenesis were selected from 4 main different groups of biological functions (A). The numbers in the parentheses represent folds of gene expression level of Cf over those in Lfs.

Table 4-1 List of top 20 common 2-fold or more up-regulated genes

Gene Common up-regulated genes	Abbreviation	Intensity of Cf	Mismatch binding	Ratio Cf/Lfs
arylacetamide deacetylase (esterase)	*DAC*	115.92	P	956.45
sparc/osteonectin (testican3)	*SPOCK3*	16.70	P	669.24
neuropeptide Y receptor Y1	*NPYR*	20.86	P	416.71
collagen, type XIV, alpha1 (undulin)	*COL14A1*	47.74	P	245.03
growth associated protein 43	*B-50*	23.52	P	232.10
procollagen C-endopeptidase enhancer 2	*PCPE2*	117.81	P	224.83
sorbin and SH3 domain containing 2	*SORB2*	10.65	P	192.25
myozenin 2	*MYOZ2*	6.53	P	139.50
serpin peptidase inhibitor, clade B (ovalbumin), member 2 transcript variant 2	*PAI2*	260.13	P	133.32
doublecortin-like kinase 1	*DCLK*	19.11	P	112.57
formyl peptide receptor-like 2	*FPRL2*	3.24	P	111.02
contactin associated protein-like 3	*CASPR3*	5.09	P	106.75
integrin, beta-like 1 (with EGF-like repeat domains)	*ITGBL1*	13.35	P	82.92
collagen, type IV, alpha 6	*COL4A6*	76.71	P	77.06
myc target 1	*MYCT1*	28.15	P	73.88
S100 calcium binding protein A4	*S100A4*	103.88	P	72.30
phosphodiesterase 1A, calmodulin-dependent	*HSPDEA1*	12.50	P	71.51
neurofilament, light polypeptide 68kDa	*NEFL*	5.71	P	69.33
ADAMTS-like 1	*ADAMTSR1*	3.24	P	68.55
early B-cell factor 1	*EBF*	4.57	P	60.80

Only those having transcripts, not EST or clones in cDNA library are listed

P = Presence of detected signal

Table 4-2 List of top 20 common 0.5-fold or less down-regulated genes

Gene Common down-regulated genes	Abbreviation	Intensity of Cf	Mismatch binding	Ratio Lfs/Cf
ST6 (alpha-N-acetyl-neuraminyl-2,3-beta-galactosyl-1,3)-N-acetylgalactosaminide alpha-2,6-sialyltransferase 5	*SIAT7E*	0.02	P	3943.41
fibrillin 2 (congenital contractural arachnodactyly)	*FBN2*	0.05	P	1035.17
fibroblast growth factor receptor 2	*FGFR2*	0.04	P	684.03
pregnancy specific beta-1-glycoprotein 5	*PSG*	0.07	P	349.77
Sal-like 1 (Drosophila)	*SALL1*	0.03	P	312.29
membrane metallo-endopeptidase	*MME*	0.05	P	274.25
odz, odd Oz/ten-m homolog 2 (Drosophila)	*TEN-M2*	0.93	P	134.10
R-spondin 3 homolog (Xenopus laevis)	*RSPO3*	0.4	P	70.16
bone morphogenetic protein 2	*BMP2A*	1.19	P	68.96
neuroligin 4, Y-linked	*NLGN4Y*	0.09	P	68.62
matrix-remodelling associated 5	*DKFZp564I1922*	1.31	P	57.89
collagen, type IV, alpha 4	*COL4A4*	0.67	P	49.71
bradykinin receptor B1	*BRADYB1*	1.61	P	48.96
microfibrillar-associated protein 4	*MFAP4*	0.3	P	32.40
matrix metallopeptidase 3 (stromelysin 1, progelatinase)	*MMP-3*	0.85	P	30.01
response gene to complement 32	*RGC32*	1.69	P	28.40
fibroblast growth factor 13	*FGF13*	0.38	P	28.15
EPH receptor A5	*EPHA5*	0.40	P	25.68
interleukin 24	*IL-24*	1.68	P	25.27

Only those having transcripts, not EST or clones in cDNA library are listed

P = Presence of detected signal

Table 4-3 Gene ontology of common up-regulated genes. Only genes in the top-five ranking of each group are shown.

Gene ontology (%)	Accession no.	Description	Cf/Lfs
Cellular metabolism	NM_000909	neuropeptide Y receptor Y1	416.71
(23.7%)	NM_004734	doublecortin-like kinase 1	112.57
	NM_002961	S100 calcium binding protein A4	72.30
	AF208502	early B-cell factor 1	60.80
	AW004016	ST6 beta-galactosamide alpha-2,6 Sialyltransferase 2	59.04
Protein binding	BF449063	collagen, type XIV, alpha 1 (undolin)	245.03
(20.8%)	NM_002045	growth associated protein 43	232.10
	AI659533	sorbin and SH3 domain containing 2	192.25
	BF939176	myozenin 2	139.5
	AF333769	contactin associated protein-like 3	106.75
Signal transduction	AW026543	formyl peptide receptor-like 2	111.02
(10.9%)	NM_004791	integrin, beta-like 1	82.92
	NM_005019	phosphodiesterase 1A	71.51
	AF159570	regulator of G-protein signalling 5	49.64
	W67461	angiopoietin-like 1	49.16
Extracellular region	NM_001086	arylacetamide deacetylase (esterase)	956.45
(7.8%)	AI808090	sparc/osteonectin, cwcv and kazal-like domains proteoglycan (testican) 3	669.24
	NM_013363	procollagen C-endopeptidase enhancer 2	224.83
	AI889941	collagen, type IV, alpha 6	77.06
	NM_052866	a disintegrin and metalloproteinase with thrombospondin motif-like 1	68.55
Transcription factor	AF332197	sine oculis homeobox homolog 2	44.20
(7.5%)	AI681917	iroquois homeobox protein 3	35.34
	NM_020639	receptor-interacting serine-threonine Kinase 4	29.41
	AK023792	PBX/knotted 1 homeobox 2	29.40
	AF208967	paternally expressed 3	26.74

Table 4-3 Gene ontology of common up-regulated genes (Cont.)

Gene ontology (%)	Accession no.	Description	Cf/Lfs
Protein modification	AW975934	titin	32.01
(5.5%)	NM_000222	v-kit Hardy-Zuckerman 4 feline sarcoma viral oncogene homolog	25.21
	BF446673	hemicentin 1	18.96
	NM_002848	protein tyrosine phosphatase, receptor type, O	14.58
	NM_001992	coagulation factor II (thrombin) receptor	13.90
Receptor	BF941499	G protein-coupled receptor 116	35.62
(4.8%)	L35594	ectonucleotide pyrophosphatase/phosphodiesterase 2	32.11
	NM_002820	parathyroid hormone-like hormone	30.44
	U61276	jagged 1 (Alagille syndrome)	19.60
	AK022548	integrin, alpha 7	15.62
Cell differentiation	AA343027	sema domain, immunoglobulin domain (Ig), short basic domain, secreted, (semaphorin) 3D	67.06
(4.3%)	NM_000216	Kallmann syndrome 1 sequence	27.91
	AL560266	Fc receptor-like A	19.61
	AA127691	neuropilin 2	19.35
	NM_002506	nerve growth factor, beta polypeptide	19.11
Cell adhesion	NM_006727	cadherin 10, type 2 (T2-cadherin)	55.43
(3.5%)	NM_000072	CD36 molecule (thrombospondin-receptor)	40.71
	AL573851	endothelial cell adhesion molecule	22.52
	N69091	protocadherin 17	22.32
	AA489646	protocadherin beta 13	19.36
Cell cycle	NM_003914	cyclin A1	34.8
(2.4%)	NM_015714	G0/G1switch 2	26.62
	NM_001759	cyclin D2	16.45
	AK024082	tousled-like kinase 2	11.09
	NM_006569	cell growth regulator with EF-hand domain 1	10.25
Cell motility	NM_005045	reelin	17.30
(2.2%)	NM_003062	slit homolog 3 (Drosophila)	5.12
	M21121	chemokine (C-C motif) ligand 5	5.06
	NM_014795	zinc finger E-box binding homeobox 2	4.85
	D45864	protein kinase, cGMP-dependent, type I	4.74

Table 4-3 Gene ontology of common up-regulated genes (Cont.)

Gene ontology (%)	Accession no.	Description	Cf/Lfs
Proteolysis	NM_001870	carboxypeptidase A3 (mast cell)	20.01
(2.0%)	NM_024539	ring finger protein 128	12.68
	AL574912	protease, serine, 35	11.59
	NM_001873	carboxypeptidase E	9.45
	NM_000892	kallikrein B, plasma (Fletcher factor) 1	6.40
Cell proliferation	U77914	jagged 1 (Alagille syndrome)	16.76
(2.0%)	NM_004624	vasoactive intestinal peptide receptor 1	13.07
	BF514079	kruppel-like factor 4 (gut)	12.89
	NM_001432	epiregulin	11.98
	BC003355	laminin, alpha 5	10.36
Apoptosis	NM_002575	serpin peptidase inhibitor	133.32
(1.6%)	NM_000557	growth differentiation factor 5	14.79
	NM_003728	unc-5 homolog C (C. elegans)	9.60
	BF432648	tumor necrosis factor receptor superfamily	8.73
	NM_003551	non-metastatic cells 5, protein expressed in (nucleoside-diphosphate kinase)	6.80
ECM organization	BC001186	protocadherin beta 5	15.90
and biosynthesis	M25813	tenascin XB	12.46
(0.9%)	NM_002380	matrilin 2	4.89
	AY140646	periostin, osteoblast specific factor 2	4.89
	NM_004612	transforming growth factor, beta receptor I (activin A receptor type II-like kinase, 53 kDa)	4.56

Table 4-4 Gene ontology of common down-regulated genes. Only genes in the top-five ranking of each group are shown.

Gene ontology (%)	Accession no.	Description	Lfs/Cf
Cellular metabolism (31.6%)	NM_030965	ST6 (alpha-N-acetyl-neuraminyl-2,3-beta-galactosyl-1,3)-N- acetylgalactosaminide alpha-2,6- sialyltransferase 5	3943.41
	NM_022969	fibroblast growth factor receptor 2	684.03
	AU152837	Sal-like 1 (Drosophila)	312.29
	NM_007287	membrane metallo-endopeptidase	73.38
	BF589322	R-spondin 3 homolog (*Xenopus laevis*)	70.16
Signal transduction (17.8%)	NM_001200	bone morphogenetic protein 2	68.96
	NM_000710	bradykinin receptor B1	48.96
	R72286	microfibrillar-associated protein 4	32.40
	NM_004114	fibroblast growth factor 13	28.15
	BE218107	EPH receptor A5	25.68
Transcription factor (11.5%)	AJ277914	LIM homeobox 9	25.01
	NM_001452	forkhead box F2	18.08
	AA705845	transducin-like enhancer of split 4 (E(sp1) homolog, Drosophila)	17.16
	BG261252	ecotropic viral integration site 1	11.58
	NM_020327	activin A receptor, type IB	9.32
Protein modification (7.9%)	AF245505	matrix-remodelling associated 5	57.89
	AA725644	ubiquitin specific peptidase 42	18.73
	NM_001982	v-erb-b2 erythroblastic leukemia viral oncogene homolog 3 (avian)	11.34
	AV727260	protein tyrosine phosphatase, receptor type, D	10.93
	NM_002570	proprotein convertase subtilisin/kexin type 6	9.83
Cell differentiation (6.2%)	NM_000641	interleukin 11	17.51
	BC006454	growth arrest-specific 7	15.20
	M69148	midkine (neurite growth-promoting factor 2)	14.03
	NM_003991	endothelin receptor type B	10.85
	AI758962	EPH receptor A4	7.15

Table 4-4 Gene ontology of common down-regulated genes (Cont.)

Gene ontology (%)	Accession no.	Description	Lfs/Cf
Cell adhesion	NM_001999	fibrillin 2	1035.17
(5.9%)	NM_014893	neuroligin 4, Y-linked	68.62
	AI694562	collagen, type IV, alpha 3	22.21
	NM_005864	embryonal Fyn-associated substrate	8.44
	AU146651	collagen, type XII, alpha 1	4.89
Cell cycle	NM_014059	response gene to complement 32	28.40
(5.9%)	M19701	retinoblastoma 1 (including osteosarcoma)	4.93
	NM_002009	fibroblast growth factor 7	4.44
	NM_014703	Vpr (HIV-1) binding protein	3.92
	AI983033	DEAD/H box polypeptide 12	3.91
Cell motility	NM_002784	pregnancy specific beta-1- glycoprotein 9	69.22
(4.7%)	X99268	twist homolog 1	5.45
	NM_015180	spectrin repeat containing, nuclear envelope 2	3.81
	AI990816	laminin, alpha 1	3.59
	N90777	neuropilin 2	3.57
Cell proliferation	NM_016931	NADPH oxidase 4	5.79
(4.5%)	AF064826	glypican 4	4.31
	NM_004525	low density lipoprotein-related protein 2	3.85
	NM_001963	epidermal growth factor (beta- urogastrone)	3.70
	AF064103	CDC14 cell division cycle 14 homolog A	3.67
Apoptosis	NM_006850	interleukin 24	25.27
(4.0%)	NM_002135	nuclear receptor subfamily 4, group A, member 1	5.48
	NM_003823	tumor necrosis factor receptor superfamily	4.59
	AJ301610	glutamate receptor, ionotropic, kainate 2	3.92
	NM_005809	peroxiredoxin 2	3.90

4.2 Gene validation and confirmation of PN expression in Cfs

The eleven up-regulated genes in Cfs which encoded secreted proteins and based on review literature shown carcinogenic properties as indicated in Figure 4-1A were selected to verify by relative quantification real time PCR. In concordance with microarray data, real time PCR results revealed that *ADAM12, AREG, ER, JAGL1, PDGF-A, PN* and *SCG2* had significant up-regulations in Cfs compared to Lfs, but that of *NOV* was not statistical significantly increased (Fig 4-2A). *ANG2, LAMA5*, and *RL*, however, showed the opposite direction to the microarray results.

PN was chosen to explore the carcinogenic effects on CCA cell lines with its critical and multifuctional roles published in various carcinomas. To ensure the up-regulation of PN in Cfs, the different biological preparation lots of Cfs from those used in microarray analysis were subjected for detection by both real time PCR and western blot analysis. The results confirmed that Cfs had higher expression of *PN* mRNA than Lfs with statistical significance (Fig 4-2B). In the same direction, PN protein level expressed in Cf was markedly higher than that Lf could produce (Fig 4-2C).

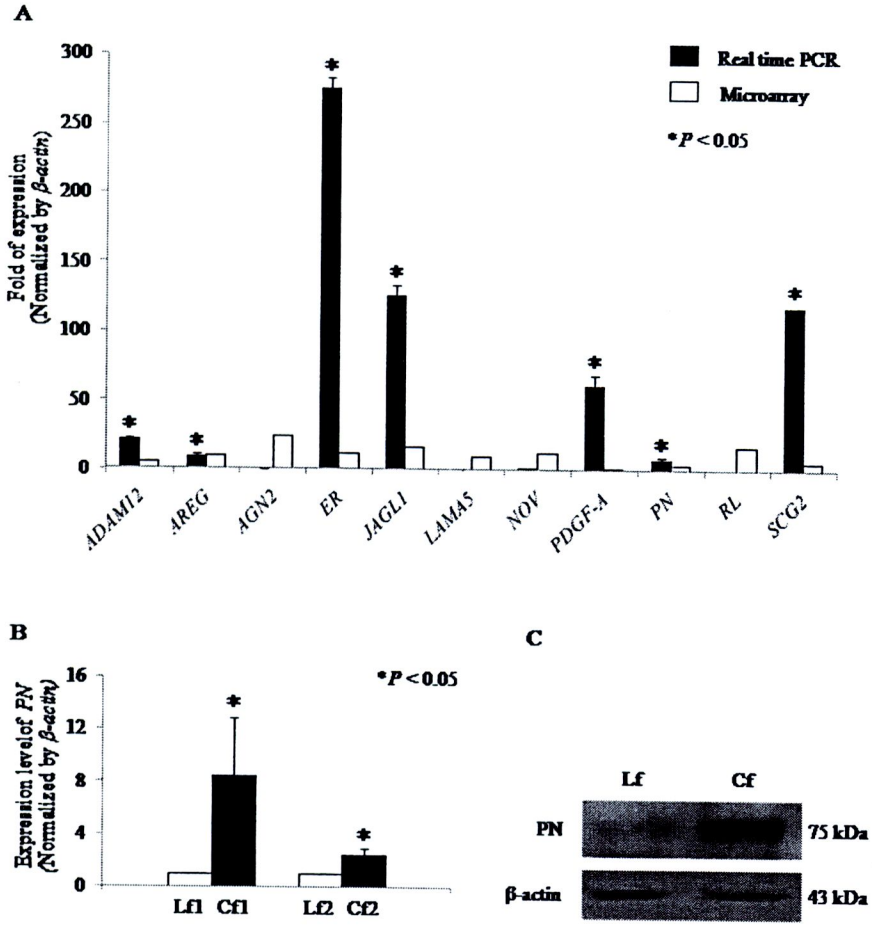

Figure 4-2 Gene validation and detection of PN in Cfs. The eleven candidate genes were validated their expression levels in Cf compared to that Lfs using real time PCR (A). The up-regulation of PN in both mRNA and protein levels was confirmed by real time PCR (B) and western blot analysis (C), respectively using different biological preparations of Cfs and Lfs from those used in microarray.

4.3 Expression of PN in CCA tissues and clinicopathological relevance

The localization of PN in CCA tissues using immunohistochemistry revealed that the expression of PN was exclusively localized in fibroblasts but not cancer cells (Fig 4-3). Moreover, double immunofluorescent staining revealed expression of PN in the surrounding area beside α-SMA-positive fibroblasts (Fig 4-4) which confirmed the activated fibroblasts as sources of PN in CCA tissues.

Of all 52 cases, 43 cases or 83% were PN positive (Table 4-5). Among these positive cases, 58% of them showed high expression levels. High expression of PN was observed in well- (Fig 4-3A), moderately- (Fig 4-3B) and poorly-differentiated malignant tissues (Fig 4-3C). For PN-negative CCA tissues, only 17% (9/52) were in this group in which no PN was detected in either fibroblasts or cancer cells (Fig 4-3D). In contrast, benign liver tissues showed no (2/8) to slight (6/8) PN expression (Table 4-5 and Fig 4-3E). Similar to benign liver tissues, hepatocellular carcinoma revealed low PN expression in their stromal cells (Table 4-5 and Fig 4-3F).

Cumulative survival of CCA patients with low or high PN expression in cancer stromal fibroblasts was analyzed. The patients with survival time under 14 d were identified as peri-operative deaths (n = 1) and excluded from the analysis. Median survival time was 395 ± 157 d for patients with low and 179 ± 35 d for patients with high PN expression. We found that the patients with high PN positive fibroblasts had statistically significantly shorter survival times than those with low PN positive fibroblasts ($P = 0.026$) (Fig 4-5). The prognostic value of PN expression and other clinicopathological factors among CCA patients was analyzed using multivariate Cox Proportional Hazard Regression model. The results revealed that high PN expression (HR = 2.02, $P = 0.045$), and the presence of lymph node metastasis (HR = 3.13, $P = 0.002$) were the independent risk factors for the overall survival of CCA patients after hepatectomy (Table 4-6). However, lymph node metastasis and other clinical data showed no association with PN expression (Table 4-7).

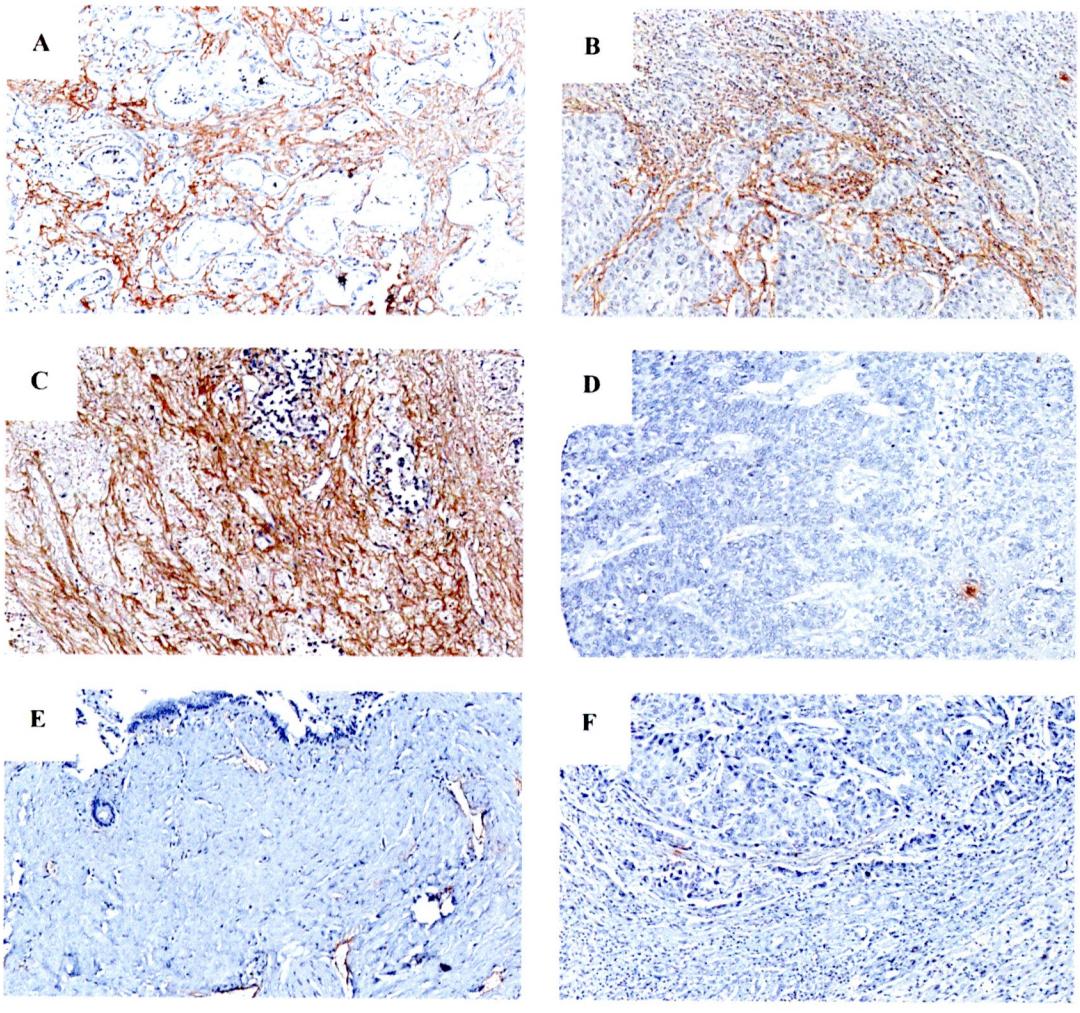

Figure 4-3 Immunohistochemical staining of PN in CCA tissues. The expression of PN was localized in fibroblasts but not cancer cells. High expression of PN was observed in well- (A), moderately- (B) and poorly-differentiated tissues (C), whereas PN negative staining CCA tissue was demonstrated (D). Benign liver tissue (E) and hepatocellular carcinoma (F) showed no to slight expression. Magnification, 100x

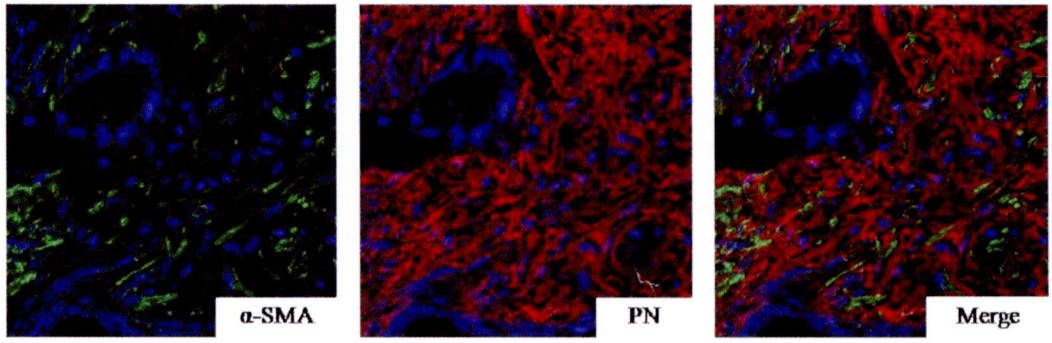

Figure 4-4 Double immunostaining of α-SMA and PN in CCA tissues. PN (red signal) secretes from α-SMA-positive-fibroblasts labled with green. Magnification, 400x.

Table 4-5 PN expression in CCA tissues compared to benign liver tissues and hepatocellular carcinoma

Tissue	Total cases (n)	PN expression in fibroblasts		
		Negative	Positive	
			Low	High
CCA	52	9 (17%)	13 (25%)	30 (58%)
Benign liver tissues	8	2 (25%)	6 (75%)	0 (0%)
Hepatocellular carcinoma	4	1 (25%)	3 (75%)	0 (0%)

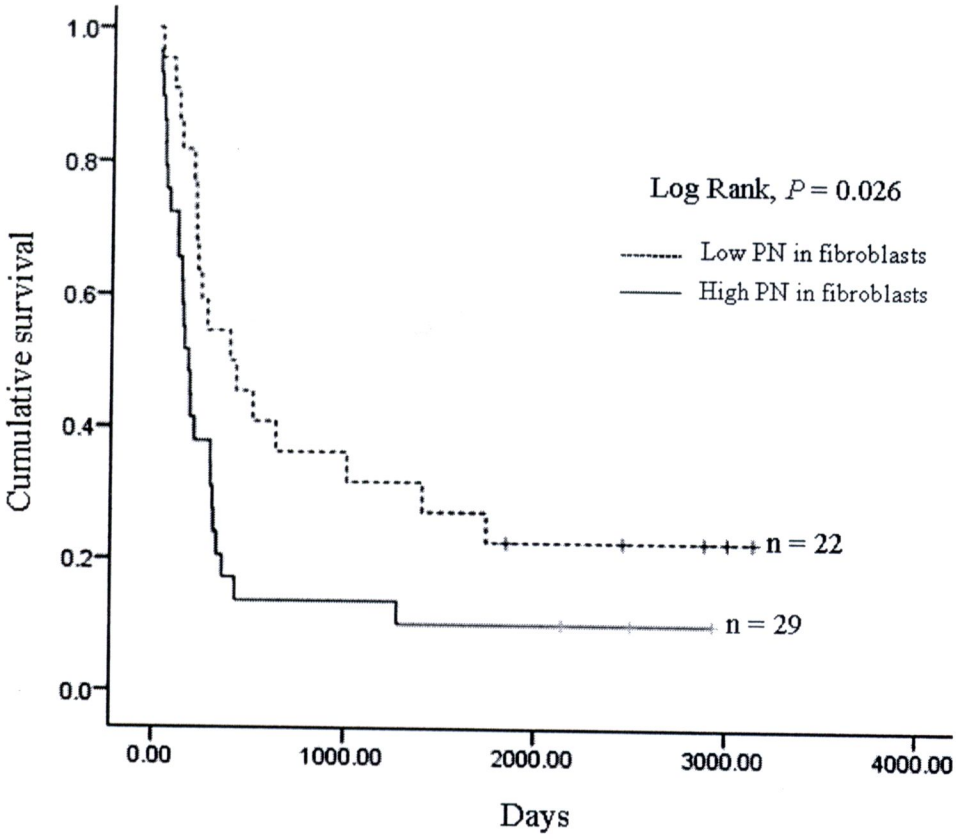

Figure 4-5 Multivariate analysis using Kaplan-Meier method. Cumulative survival analysis showed significantly shorter survival time of the patients with high PN expression in fibroblasts when compared to those who had low PN expression in fibroblasts (P =0.026).

Table 4-6 Multivariate analysis by Cox Proportional Hazard Regression model for the evaluation of prognostic factors

Variable (No. of patients)	No. of dead patients (5-yr survival cut-off)	HR (Hazard ratio)	95% Confidence interval (CI)	*P*
Age in years				
≤57 (25)	21	1		
>57 (26)	22	1.25	0.62-2.48	0.533
PN expression				
Low (22)	17	1		
High (29)	26	2.02	1.02-4.02	0.045*
Lymph node metastasis				
Absence (36)	28	1		
Presence (15)	15	3.13	1.54-6.35	0.002*
Histological type				
Well-differentiated (20)	16	1		
Moderately-differentiated (8)	8	2.77	1.10-6.98	0.031*
Poorly-differentiated (8)	7	1.64	0.63-4.29	0.310
Papillary (15)	12	0.60	0.25-1.44	0.254
Tumor size (cm)				
≤5 (28)	23	1		
>5 (23)	20	1.49	0.76-2.94	0.251

* *P* value of less than 0.05 means statistical significance

Table 4-7 Correlation between PN expression level and clinicopathological parameters

Variable	n	PN expression (%)		Univariate analysis	Multivariate analysis	
		Low	High	*P*	HR	*P*
Age in years				0.575		
≤57	26	10 (38.5)	16 (61.5)		1	
>57	26	12 (46.2)	14 (53.8)		0.899	0.870
Sex				0.375		
Female	20	10 (50.0)	10 (50.0)		1	
Male	32	12 (37.5)	20 (62.5)		1.638	0.452
Histological type				0.083		
Well-differentiated	21	8 (38.1)	13 (61.9)		1	
Moderately-differentiated	8	1 (12.5)	7 (87.5)		3.720	0.271
Poorly-differentiated	8	6 (75.0)	2 (25.0)		0.184	0.86
Papillary	15	7 (46.7)	8 (53.3)		0.611	0.505
Tumor size (cm)				0.123		
≤5	29	15 (51.7)	14 (48.3)		1	
>5	23	7 (30.4)	16 (69.6)		2.493	0.161
Lymph node metastasis				0.830		
Absence	37	16 (43.2)	21 (56.8)		1	
Presence	15	6 (40.0)	9 (60.0)		1.459	0.590

4.4 PN promotes proliferation and invasion of CCA cells

In order to know the impact of fibroblast-derived PN in CCA, tumorigenic properties including cell proliferation and invasion of CCA cell line induced by PN were explored. The result showed that PN could induce proliferation of CCA cell lines; KKU-M156, KKU-M213 and KKU-M055 (Fig 4-6A-C), but not KKU-100 (Fig 4-6D). All 3 CCA cell lines; KKU-M156, KKU-M213 and KKU-M055, responded to the proliferative effect of 100 ng/ml recombinant PN. In addition, PN induced CCA cell proliferation in a time dependent manner with statistical significance at the 24-h treatment for these 3 cell types (Fig 4-7). Since the unresponsiveness to PN stimulation, KKU-100 was not be included in the later experiments.

Flow cytometric analysis indicated an increased number of KKU-M213 and KKU-M156 cells distributed in S+G2/M when exposed to PN (34 ± 11% in KKU-M213 and 44 ± 8% in KKU-M156) compared to those of without PN induction (29 ± 9% in KKU-M213 and 37 ± 4% in KKU-M156) (Fig 4-8A and B).

To reinforce the effect of PN to induce cancer cell growth *in vitro*, the anchorage growth-independent and anchorage growth-dependent were performed by colony formation assay with and without soft agar, respectively. The result indicated the increased number of colonies in soft agar with PN treatment (56 ± 4 colonies for KKU-M213 and 39 ± 4 colonies for KKU-M156) in comparison to the negative control without PN stimulation (43 ± 1 colonies for KKU-M213 and 30 ± 1 colonies for KKU-M156) (Fig 4-9). The increasing number of colonies in the condition of PN treatment were confirmed in that of culturing in the system without soft agar (114 ± 11 colonies for KKU-M213 and 116 ± 30 colonies for KKU-M156) in comparison to the negative control (97 ± 2 colonies for KKU-M213 and 91 ± 27 colonies for KKU-M156) (Fig 4-9).

The results altogether confirmed that exogenous PN was able to induce CCA cell proliferation and cancer growth.

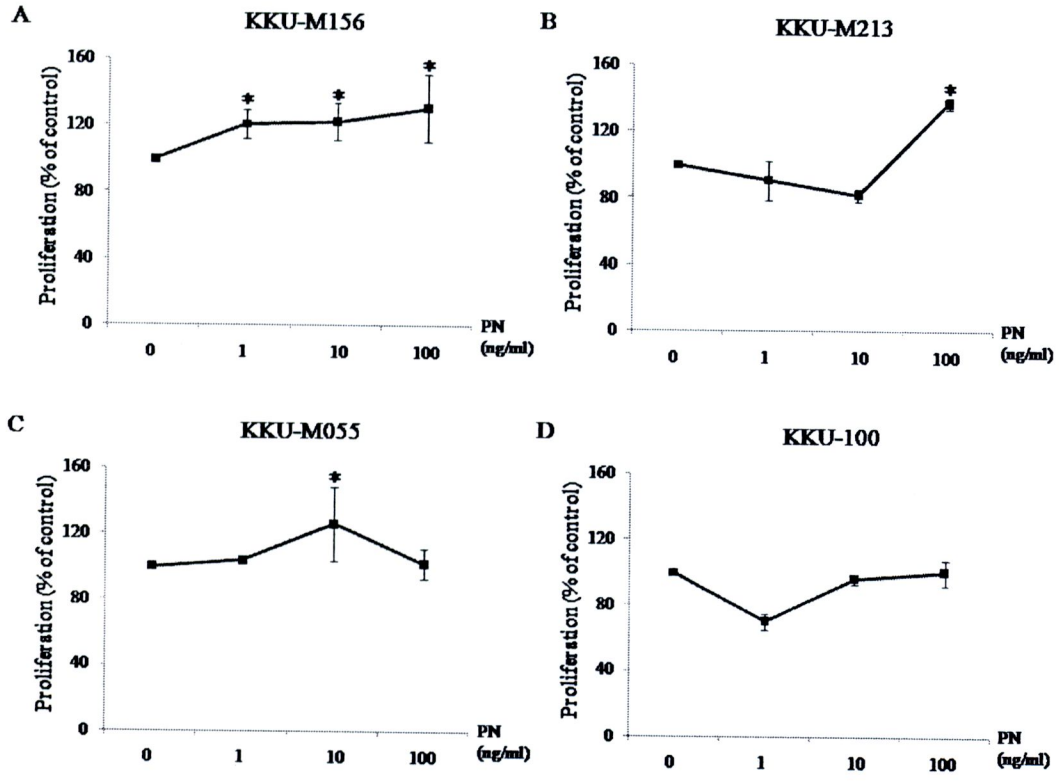

Figure 4-6 PN-activated proliferation of CCA cell lines. KKU-M156, KKU-M213 and KKU-M055 showed significantly induced proliferation with different doses of PN (A-C) whereas KKU-100 was unresponsive to PN (D). Results are expressed as mean ± SD and an asterix represents a *P* value less than 0.05 when compared to the negative controls without PN treatment which were adjusted to be 100%.

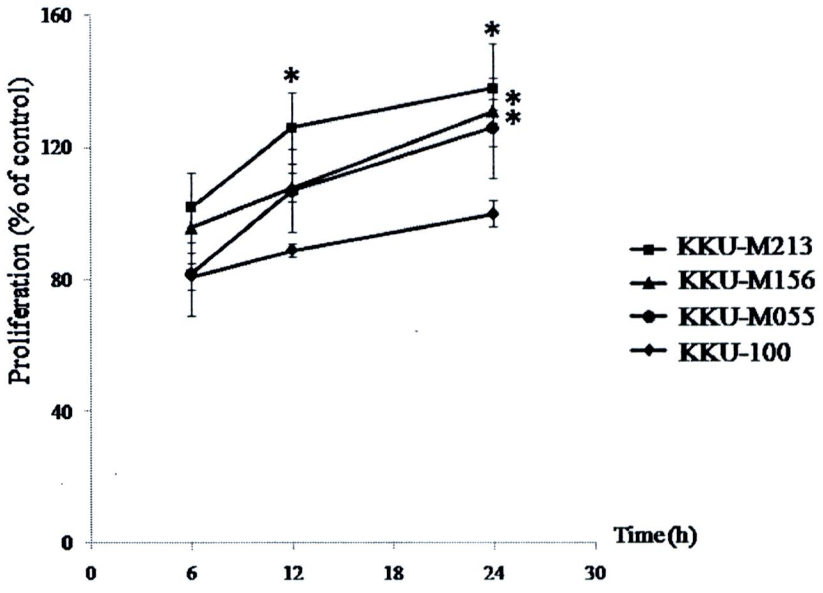

Figure 4-7 PN-induced proliferation in a time-dependent manner. KKU-M213, KKU-M156, KKU-M055 and KKU-100 were treated with 100 ng/ml PN for various time points. Triplicate experiments were performed for each assay. Results are expressed as mean ± SD and an asterix represents a *P* value of less than 0.05 when compared to the negative controls without PN treatment.

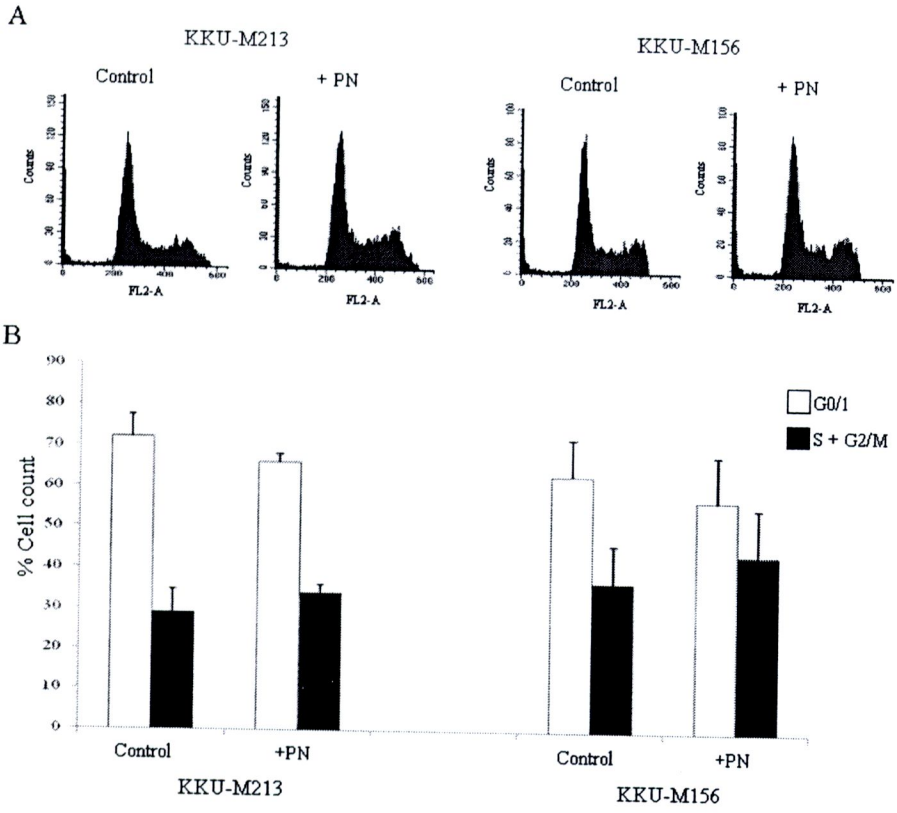

Figure 4-8 Cell cycle distribution analysis of cancer cells with and without stimulation by PN. Histogram plots represent the correlation of PI signal (FL-2A) and numbers of cells (A). PN could drive cells from G1 into S and G2/M phases of the cell cycle when compared to control cells without PN treatment showing by the percentage of cells in G0/1 and S+G2/M of the cell cycle (B).

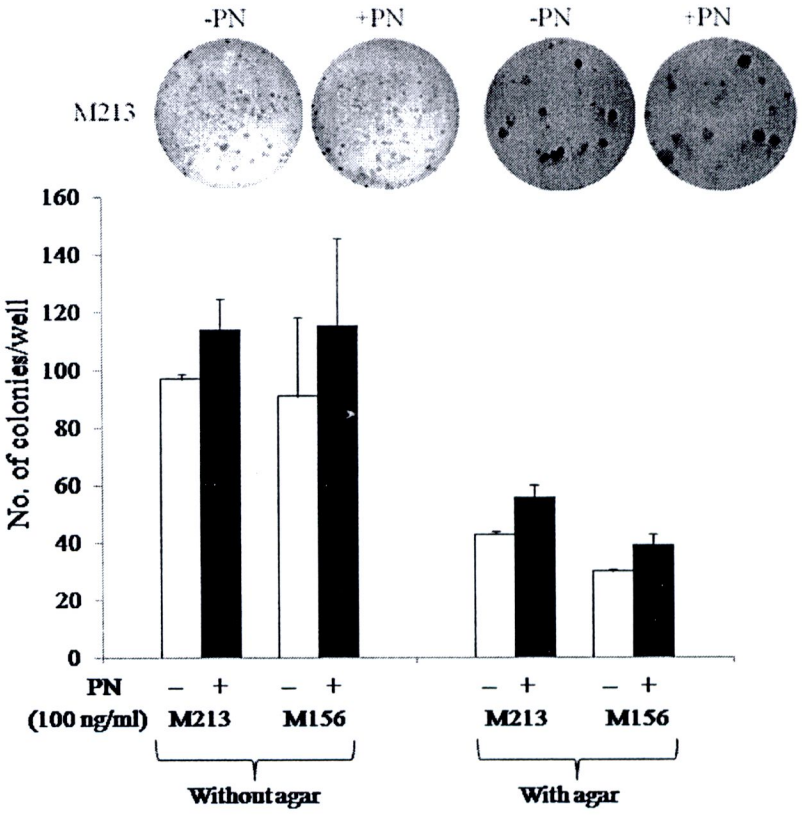

Figure 4-9 PN promotes CCA cell growth. Colony formation assay with and without soft agar was performed using KKU-M213 and KKU-M156. Colony of more than 30 cells was counted under inverted microscope. Bars are expressed as mean ± SD of duplicate experiments. Pictures of crystal violet-stained cells are of KKU-M213 CCA cells in comparison between with and without PN.

To address the invasive effect of PN on CCA cells, the double chamber invasion assay using Boyden chamber showed that exogenous PN could markedly induce invasion of KKU-M213 and KKU-M156 CCA cell lines up to around 247 ± 5% and 214 ± 5%, respectively compared to cells without PN treatment (Fig 4-10). The intrinsic invasiveness of parental KKU-M213 and KKU-M156 was around 6 ± 3 cells and 7 ± 4 cells, respectively. However, number of invaded cells increased to 14 ± 3 cells for KKU-M213 and 15 ± 8 cells for KKU-M156. These result indicated that, in addition to proliferation induction, PN could activate CCA cell invasion.

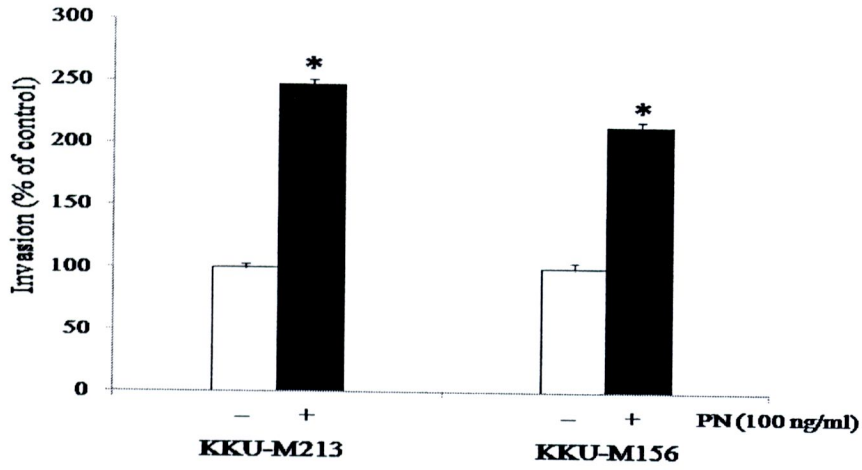

Figure 4-10 Invasion induction by PN on KKU-M213 and KKU-M156 CCA cell lines. Number of invaded cells when no PN in the culture media was served as negative control were adjusted to be 100% (white bars). Black bars represent invaded cells after stimulation by PN shown as percentage of cells in comparison to that of the negative control. Each bar represents mean ± SD of three independent experiments. An asterix represents a *P* value of less than 0.05.

4.5 Integrin alpha 5 expression on biliary epithelial and CCA cells

To explore the mechanism that PN utilizes to activate aggressive tumorigenic characters of CCA, expression of ITGs which known as PN receptors was explored. In this study, ITGα5 was revealed the expression on both tumorigenic biliary epithelial cells; KKU-M213, KKU-M214, KKU-M055, KKU-OCA17, KKU-100, KKU-M156, and KKU-M139; and MMNK1 non-tumorigenic biliary epithelial cells. Using flow cytometry analysis, the relative mean fluorescence intensity (MFI) showed high level of ITGα5 in KKU-M213 cell line (MFI = 2.0 ± 0.57) which in the previous experiment showed high response to PN-stimulated cell proliferation and invasion (Fig 4-7 and Fig 4-10) compared to that of KKU-100 (MFI = 1.5 ± 0.21) which did not respond to PN (Figure 4-7). However, levels of ITGα5 in KKU-M156 (MFI = 1.4 ± 0.09) and KKU-M055 (MFI = 1.6 ± 0.26) were quite near to that of KKU-100. For the rest of cells studied herein including KKU-M214, KKU-OCA17, KKU-M139, and MMNK1, the results revealed nearly the same level of ITGα5 to that found in KKU-M156.

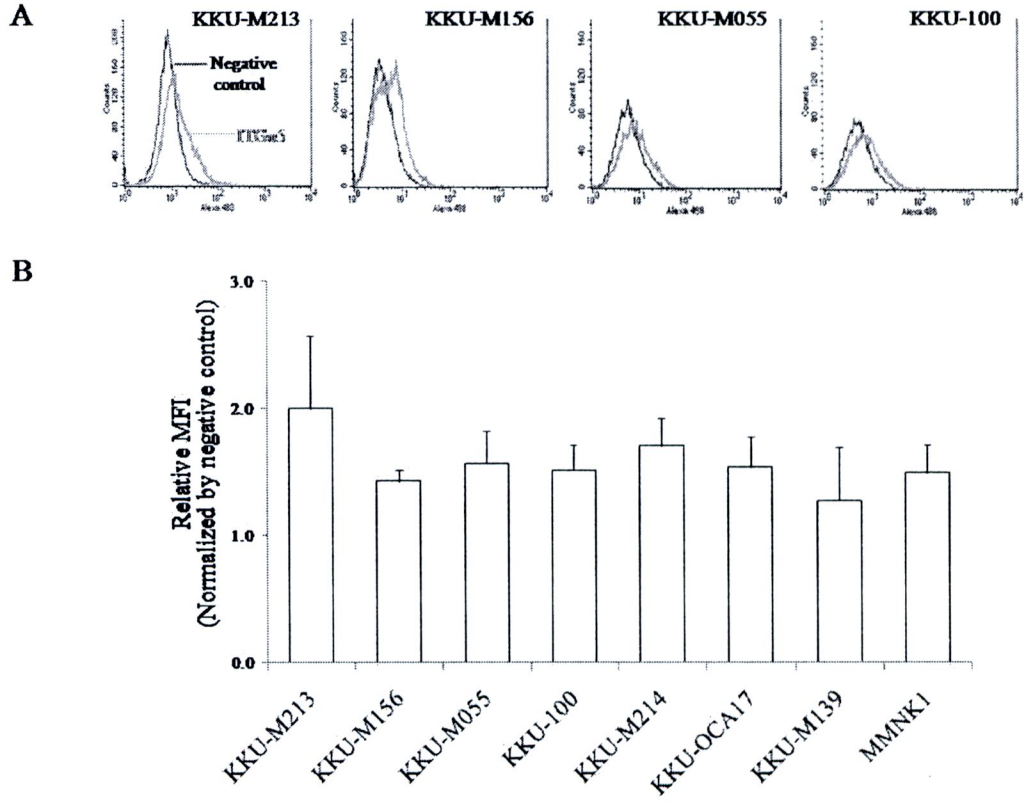

Figure 4-11 The expression of ITGα5 on biliary epithelial cells. Histogram plots represent the correlation of ITGα5 (Alexa 488) signal (FL-1) and numbers of cell count measured by flow cytometry (A). The result is shown as MFI of ITGα5 in each cell line normalized by the negative control (without primary antibody staining) (B). Each bar graph represents mean ± SD of two independent experiments.

4.6 ITGα5 mediates PN-induced proliferation and invasion

To know whether ITGα5 involves in PN-activated CCA cell proliferation and invasion, si*ITGα5*-treated CCA cells were produced. Treatment of CCA cells including KKU-M213 and KKU-M156 with si*ITGα5* and lipofectamine (mock) for 6 h did not affect cell viability (Fig 4-12A). The *ITGα5*-knockdown KKU-M213 cells could be detected the decreased *ITGα5* mRNA level up to 72 h after siRNA treatment (data not shown). Thus, the subsequent investigations of cell proliferation and invasion could be performed within 72 h after transient knockdown with si*ITGα5*. The reduction of *ITGα5* expression was observed around 86% in KKU-M213 and 69% in

KKU-M156 CCA cells with siRNA treatment for 24 h compared to that in control cells without PN treatment which assumed to the 100% (Fig 4-12B).

The data revealed that the reduction of *ITGα5* expressions in both KKU-M213 and KKU-M156 CCA cells resulted in a significant decreased response of cells to PN-induced cell proliferation and invasion (Fig 4-12C and D). A 104 ± 0% of KKU-M213 cell proliferation induction was detected in si*ITGα5*-treated cells exposed to PN, whereas cell proliferation could be increased up to 130 ± 7% in cells with intrinsic *ITGα5* expression (Fig 4-12C). In the same manner, KKU-M156 showed 118 ± 16% and 98 ± 0% of cell proliferation induction observed in cells untreated and treated with si*ITGα5*.

The *ITGα5*-knockdown CCA cell lines did not respond to PN-activated cell invasion (100 ± 0% for KKU-M213 and 100 ± 8% for KKU-M156) whereas PN dramatically induced invasion of both cell lines having normal intrinsic *ITGα5* expression (172 ± 2% for KKU-M213 and 168 ± 1% for KKU-M156) (Fig 4-12D). Taken the results together, it was suggested that PN might activate CCA cell proliferation and invasion via ITGα5-mediated pathway.

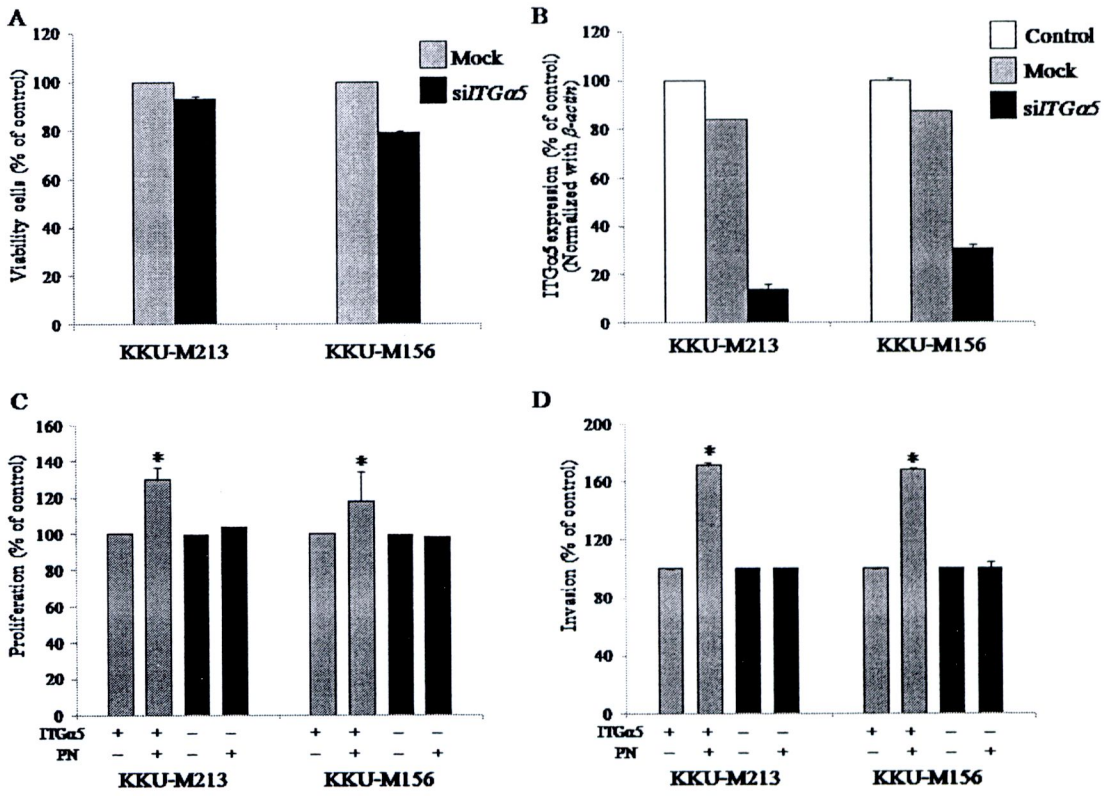

Figure 4-12 Effect of si*ITGα5* on PN-induced proliferation and invasion of CCA cells. Lipofectamine-treated cells (mock) had nearly the same viability as si*ITGα5* treated cells (A). KKU-M213 and KKU-M156 showed dramatically decreased expression of *ITGα5* detected by real time PCR after exposure to si*ITGα5* (B). Percentage of proliferation and invasion compared to control mock cells is shown. The si*ITGα5*-treated cells (negative ITGα5) could not respond to PN in induction of proliferation as much as that detected in cells without exposure to si*ITGα5* (positive ITGα5) (C). A similar effect was observed in PN-induced invasion of CCA cell lines (D). Results represent mean ± SD of three independent experiments and, an asterix represents significantly increased cell proliferation and invasion by PN of mock cells compared to those without PN treatment and significantly decreased cell proliferation and invasion of si*ITGα5*-treated cells compared to mock cells after PN treatment, respectively ($P < 0.05$).

4.7 ITGα5β1 receptor-mediated CCA invasion induced by PN

Since PN-induced cancer cell invasion revealed dramatic change from control (Fig 4-10) more than PN-induced cell proliferation (Fig 4-7), we selected to explore in depth the role and mechanism of ITGα5-mediated PN-induced cell invasion. ITGα5 normally synthesized and formed with ITGβ1 to receive ITGα5β1 heterodimer acting as a functional receptor on cell membrane. To ensure role of this receptor in PN-induced CCA invasion, intact ITGα5β1 on KKU-M213 cell membrane was blocked with anti-ITGα5β1 antibody before exposure to PN. The result revealed that CCA cells with intrinsic expression of ITGα5β1 had around 24 invaded cells which assumed to be 100% invasion (Fig 4-13). These parental cells were induced invasion by PN up to 246% (59 invaded cells). However, when the cells were blocked with anti-ITGα5β1 antibody, the intrinsic invasion was decreased to be 38 ± 6% (9 ± 6 invaded cells). Interestingly, after PN induction, the ITGα5β1-blocked cells showed invasive capability to be 44 ± 9% which was the similar level of anti-ITGα5β1-antibody-treated cells without PN exposure (Fig 4-13). These results implied the essential of ITGα5β1 for intrinsic and PN induced invasion.

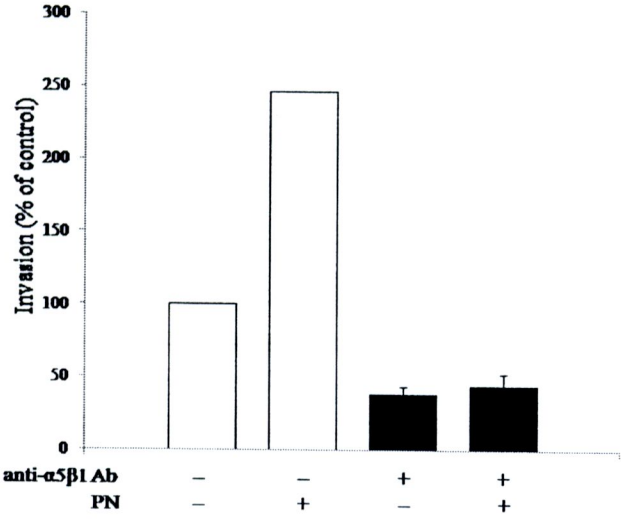

Figure 4-13 Neutralization of intact ITGα5β1 receptor attenuates PN-induced CCA cell invasion. KKU-M213 cells were incubated with anti-α5β1 antibody prior to treat with 100 ng/ml PN for 24 h. The data revealed percentage of invaded cells induced by PN compared to that of the parental cells without PN treatment which assumed to be 100%. Bar shows mean ± SD of duplicate wells in one experiment.

4.8 PN promotes CCA cell invasiveness via ITGα5β1 and AKT signaling pathway

In order to investigate whether PN-ITGα5β1 ligation activates AKT or ERK dependent signal pathway leading to cell invasion, KKU-M213 CCA cell line was knockdown the expression of *ITGα5* before stimulation with PN, and pAKT and pERK1/2 were measured compared to those of mock cells.

The ITGα5 immunofluorescent staining result showed the depletion of intact ITGα5β1 receptor on the membrane of CCA cells after si*ITGα5* treatment (Fig 4-14A). By adjustment of invading cells with intrinsic ITGα5 expression as 100% (412 ± 0 invaded cells), PN significantly induced invasion of these parental cells to 156 ± 18% (644 ± 33 invaded cells) (Fig 4-14B). The ITGα5-knockdown cells showed no change of their invasive capability (118 ± 21%; 488 ± 21 invaded cells). Moreover, PN could not induce invasion of the ITGα5-knockdown cells (126 ± 9%; 519 ± 9 invaded cells). This result confirms the decreased PN-induced invasion to that observed in anti-ITGα5β1-antibody-treated cells (Fig 4-13).

For the activation of downstream signal molecules inside the cells, PN could induce level of pAKT in CCA cells after 120-min treatment (Fig 4-14C). ITGα5-knockdown cells which had low responsiveness to PN-induced cell invasion showed the decreased level of pAKT compared to the mock cells having high responsiveness to PN-induced cell invasion after stimulation with PN for 30 and 120 min (Fig 4-14C). However, level of pERK1/2 did not change when compared between cells with and without transient ITGα5-knockdown cells. These results suggested that upon PN-stimulated ITGα5β1, AKT, but not ERK, was activated as the downstream signal molecule. Hence, AKT may be an intracellular signal molecule for transducing PN-activation through ITGα5β1 receptor and play important role in CCA invasion.

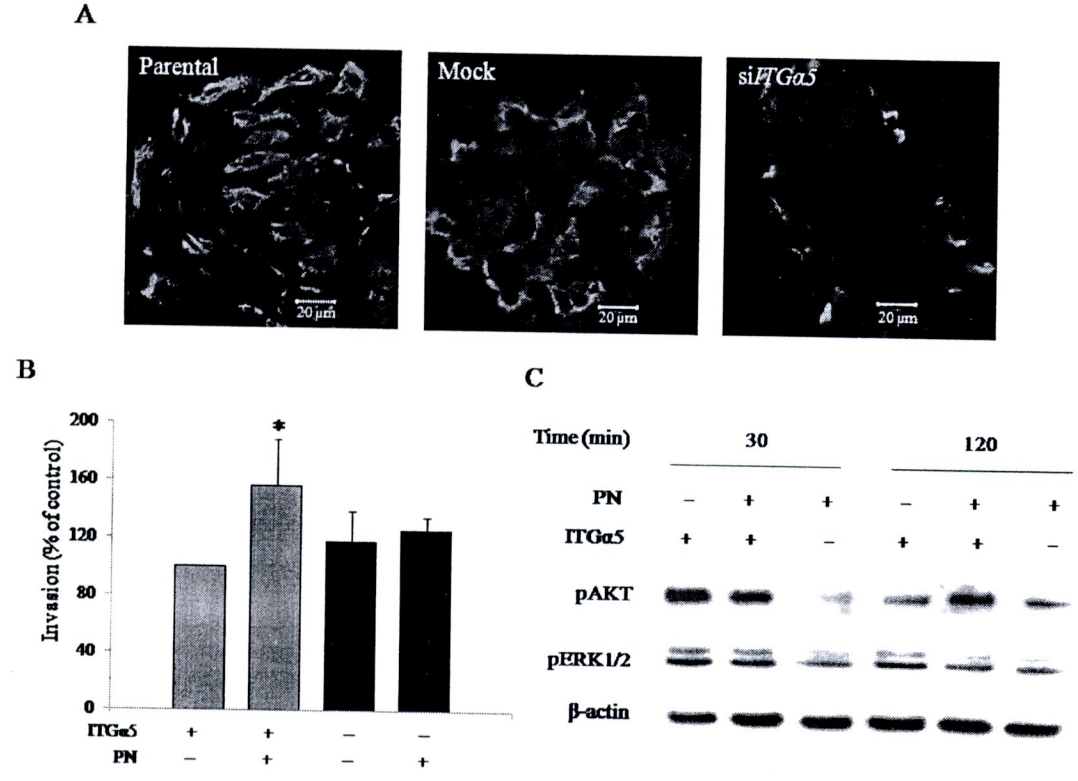

Figure 4-14 PN-induced invasion via ITGα5 and AKT signaling pathway. Depletion of ITGα5β1 receptor was observed in si*ITGα5*-treated cells by immunofluorescent staining (A). PN-induced invasion of si*ITGα5*-treated cells (negative ITGα5) and mock cells (positive ITGα5) are shown (B). The graph shows percentage of invaded cells after exposure to PN compared to that of no PN treatment which assumed to be 100%. Bar represents mean ± SD of duplicate wells in one experiment. An asterix represents significantly ($P < 0.05$) increased cell invasion induced by PN of mock cells compared to control. Western blot analysis shows level of pAKT and pERK1/2 in si*ITGα5*-treated cells and mock cells after treated with 100 ng/ml of PN for 30 and 120 min (C). The β-actin level indicates equal amount of loading protein.